Acoustic radiation force of a free spherical particle in a bounded viscous fluid

LIU Teng[1], QIAO Yupei[2, *], GONG Menyang[3], LIU Xiaozhou[1, *]

1.Key Laboratory of Modern Acoustics, Institute of Acoustics and School of Physics, Nanjing University, Nanjing 210093, China

2.School of Physics and Electronic Science, Guizhou Normal University, Guiyang 550025, China

3.School of Electronic and Information Engineering, Nanjing University of Information Science and Technology, Nanjing 210044, China

[*]

Abstract

The manipulation of particles by acoustic radiation force (ARF) has the advantages of non-invasiveness, high biocompatibility, and wide applicability. The study of acoustic radiation force is an important foundation for improving the accuracy and effectiveness of particle manipulation technology. Based on the acoustic wave theory, a theoretical model for the ARF of a free spherical particle in a bounded viscous fluid is established. The ARF for the case of a normal incident plane wave is derived by applying the translation addition theorem to spherical function. The dynamic equation of a free sphere is required as a correction term for calculating the ARF. The effects of the fluid viscosity, particle material, particle distance from boundary, and the boundary on the ARF are analyzed by numerical simulation. The results show that the resonance peak of the ARF curve is broadened with the increase of the viscosity of the fluid. Compared with the values of the ARFs of a PE sphere in a viscous and an ideal fluid, the fluid viscosity has a small influence and the viscosity effect can be ignored when *kR* is much less than 1. However, for the cases where *kR* is greater than or equal to 1, the amplitude of the ARF experienced by a particle in a viscous fluid is much greater than that in an ideal fluid. The influence of fluid viscosity on the ARF is significant and cannot be ignored. Moreover, compared with a liquid material sphere, the oscillation of ARF in an elastic material sphere is more pronounced. This is because the momentum transfer between sound waves and elastic materials is greater than that between sound waves and liquid materials. In addition, the amplitude of

---

[*] The paper is an English translated version of the original Chinese paper published in *Acta Physica Sinica*. Please cite the paper as: LIU Teng, QIAO Yupei, GONG Menyang, LIU Xiaozhou, LIU Teng, QIAO Yupei, GONG Menyang, LIU Xiaozhou, Acoustic radiation force of a free spherical particle in a bounded viscous fluid. *Acta Phys. Sin.* 2025, 74(1): 014301.
doi: 10.7498/aps.74.20241354

the ARF increases with the increase of the reflection coefficient of the impedance boundary, but its resonance frequency is not affected. Finally, the position of the sphere mainly affects the oscillation phenomenon of its ARF. The peaks and dips of the ARF become more densely packed with the growth of distance-to-radius. It is worth noting that the reflection coefficient mainly affects the amplitude of the ARF, while the position of the sphere affects the period of the ARF function. The results indicate that more efficient manipulation of particles can be achieved through appropriate parameter selection. This study provides a theoretical basis for acoustically manipulating a free particle in a bounded viscous fluid and contributes to the better utilization of ARF for particle manipulation in biomedical and other fields.

Keywords: viscous fluid, free spherical particle, acoustic radiation force, impedance boundary

PACS:

43.25.+y (Nonlinear acoustics)

43.35.+d (Ultrasonics, quantum acoustics, and physical effects of sound)

doi: 10.7498/aps.74.20241354
cstr: 32037.14.aps.74.20241354

1. Introduction

Acoustic radiation force (ARF) is a nonlinear effect of sound field, which is the result of momentum transfer between the sound field and the object. ARF manipulation has the advantages of non-invasive, wide applicability, and controllable particle scale span, so it has a wide range of applications in biomedicine, material science and other fields [1,2]. This also requires higher accuracy and effectiveness of particle manipulation technology, making study on ARF particularly important. In 1934, King [3] proposed the concept of ARF and investigated the ARF on a rigid sphere in an ideal fluid. Based on this, Hasegawa and Yosioka [4] considered the elasticity of a particle, and calculated the ARF on an elastic sphere in an ideal fluid. In addition to plane waves, the ARFs on a particle in new types of sound fields such as Bessel waves, Gaussian waves, Mathieu waves and standing waves have also been studied [5–12]. Recently, Gong et al. [13] achieved the generation of negative ARF through the acoustic field generated by a resonant adhesive structure, and the variation of the ARF with the incident acoustic frequency and various parameters of the resonant adhesive structure is discussed and explained in detail. Then a scheme of realizing negative ARF based on a multi-layer spherical structure is proposed, and the negative ARF is realized by suppressing the backscattering [14]. Gaunaurd and Huang [15] introduced the effect of a boundary and analyzed the scattering of a plane wave by a spherical particle near the boundary by combining with the method of images. In order to combine with the application of contrast agents near a blood vessel wall in medical ultrasound, Miri and Mitri[16] established a theoretical model for the ARF of an elastic spherical shell in an ideal fluid near a non-rigid boundary, and analyzed and discussed the ARF of a spherical particle made of elastic polyethylene material in detail. Westervelt[17] first considered the influence of fluid viscosity on ARF in practical application and calculated the ARF on a fixed spherical particle. Doinikov [18] provided a theoretical analysis of the ARF of a free sphere in a viscous fluid and studied the ARF of a viscous compressible liquid sphere in the strong and weak dissipation limits. Qiao et al. [19] calculated the ARF of a free spherical particle in a viscous fluid and the expression of the ARF is applicable to fluids with arbitrary viscosity. Taking polystyrene spherical particles as an example, the ARF was quantitatively measured through experiments. In practical application scenarios in biomedicine and other fields, in order to improve the accuracy and effectiveness of ARF manipulation, multiple factors such as fluid viscosity, particle free state, boundary and particle position need to be considered simultaneously. In this paper, the expression of the ARF experienced by a free spherical particle in a bounded viscous fluid is derived under the condition of plane wave perpendicular boundary incidence, and the influence of various factors on the ARF is analyzed.

2. Theoretical derivation

2.1 Model building

Consider a free spherical particle with a radius of R located near an impedance boundary in a viscous fluid. The impedance boundary is treated as a local reaction boundary (the motion at a given point on the surface is only related to the sound pressure incident on that part, and is independent of the motion of any other part of the surface), and its physical properties are represented by using the boundary reflection coefficient R_s [16]. The distance from the center of the particle to the boundary is d. A Cartesian coordinate system (x, y, z) and a spherical coordinate system (r, θ, φ) centered on a spherical particle O are established respectively, as shown in Fig. 1. The axis Ox is perpendicular to the boundary and the plane wave is along the Ox. According to the method of images, an image particle (with the same size, material, and distance from the boundary as the original particle) and an image acoustic source (an image plane wave with the same amplitude but opposite direction as the original incident plane wave) are introduced in the image space on the other side of the boundary, as shown in Fig. 1. For theoretical analysis, a Cartesian coordinate system (x_1, y_1, z_1) and a spherical coordinate system $(r_1,\ \theta_1,\ \varphi_1)$ centered on a spherical particle O_1 are established respectively.

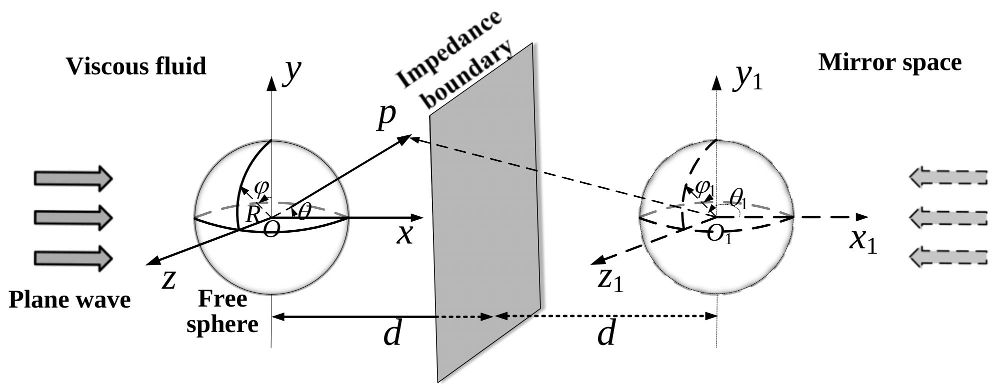

Figure 1. Schematic diagram of a free spherical particle in a bounded viscous fluid with a plane wave incidence.

In the spherical coordinate system $(r,\ \theta,\ \varphi)$, the velocity potential of the incident plane wave is expressed as

$$\phi_{\mathrm{i}}=\sum_{n=0}^{\infty}A(2n+1)\mathrm{i}^{n}\mathrm{j}_{n}(\alpha r)\mathrm{P}_{n}(\cos\theta)\mathrm{e}^{-\mathrm{i}\omega t}, \quad (1)$$

where $A=\sqrt{2I_0/\rho_0c_0k^2}$ is the incident wave amplitude, I_0 is the incident wave acoustic energy, ρ_0 is the viscous fluid density, c_0 is the speed of sound in the fluid, $k=\mathrm{Re}(\alpha)$, $\alpha=(\omega/c_0)\left[1-\mathrm{i}\omega(\lambda'+2\mu')/\rho_0c_0^2\right]^{-1/2}$ is the longitudinal wave number in the viscous fluid, ω is the acoustic wave incident angular frequency, $\mathrm{j}_n(\cdot)$ is the nth-order spherical Bessel function, $\mathrm{P}_n(\cdot)$ is the nth-order Legendre function, $\lambda'=\eta'-2\mu'/3$, μ' is the dynamic viscosity coefficient, η' is the second viscosity coefficient or the volume expansion viscosity coefficient. For most fluids, the volume expansion is not very large and is generally taken as $\eta'\approx 0$, then $\lambda'=-2\mu'/3$, which is applicable in many applications [20].

Scattering of sound waves from a spherical particle into a viscous fluid with scattered longitudinal waves ϕ_{s} and scattered transverse wave ψ_{s}. The scattering wave equation for a particle in spherical coordinate system $(r,\ \theta,\ \varphi)$ is

$$(\Delta+\alpha^2)\phi_s = 0, \tag{2}$$

$$(\Delta+\beta^2)\psi_s = 0, \tag{3}$$

where $\beta = (1+\mathrm{i})/\delta$ is the scattered shear wave number, $\delta = \sqrt{2\mu'/\rho_0\omega}$ is the viscous boundary layer and represents the penetration depth of the viscous wave.

In spherical coordinate system $(r,\ \theta,\ \varphi)$, solving the equation (2) and equation (3) the scattering wave velocity potentials of the particle can be obtained:

$$\phi_s = \sum_{n=0}^{\infty} A_n (2n+1)\mathrm{i}^n \mathrm{h}_n^{(1)}(\alpha r)\mathrm{P}_n(\cos\theta)\mathrm{e}^{-\mathrm{i}\omega t}, \tag{4}$$

$$\psi_s = \sum_{n=0}^{\infty} B_n (2n+1)\mathrm{i}^n \mathrm{h}_n^{(1)}(\beta r)\frac{\mathrm{d}}{\mathrm{d}\theta}\mathrm{P}_n(\cos\theta)\mathrm{e}^{-\mathrm{i}\omega t}, \tag{5}$$

where A_n and B_n are the scattering coefficients determined by the boundary conditions, $\mathrm{h}_n^{(1)}(\cdot)$ is the *n*th-order spherical Hankel function of the first kind.

According to the method of images, the reflection of the sound waves by the boundary is transformed into the scattering waves of the mirror sound source and the mirror particle, and their velocity potentials are expressed in the corresponding coordinate system as

$$\phi_{\mathrm{ref}} = A\sum_{n=0}^{\infty} R_s \exp(\mathrm{i}2\alpha d)(-1)^n(2n+1)\mathrm{i}^n \mathrm{j}_n(\alpha r)\mathrm{P}_n(\cos\theta), \tag{6}$$

$$\phi_{\mathrm{s,ref}} = \sum_{n=0}^{\infty} R_s(-1)^n(2n+1)\mathrm{i}^n A_n \mathrm{h}_n^{(1)}(\alpha r_1)\mathrm{P}_n(\cos\theta_1), \tag{7}$$

$$\psi_{\mathrm{s,ref}} = \sum_{n=0}^{\infty} R_s(-1)^n(2n+1)\mathrm{i}^n B_n \mathrm{h}_n^{(1)}(\beta r_1)\frac{\mathrm{d}}{\mathrm{d}\theta}\mathrm{P}_n(\cos\theta_1), \tag{8}$$

where R_s is the sound pressure reflection coefficient of the boundary, and the limit values of the reflection coefficient $R_s = +1$ and $R_s = -1$ correspond to the rigid and compliant boundaries respectively.

When dealing with the mirror particle, the additive theorem of spherical function [21, 22] is used to rewrite the scattered waves (7) and (8) as

$$\phi'_{\mathrm{s,ref}} = \sum_{n=0}^{\infty}\sum_{m=0}^{\infty} R_s(-1)^m(2m+1)\mathrm{i}^m A_m Q_{mn}\mathrm{j}_n(\alpha r)\mathrm{P}_n(\cos\theta), \tag{9}$$

$$\psi'_{\mathrm{s,ref}} = \sum_{n=0}^{\infty}\sum_{m=0}^{\infty} R_s (-1)^m (2m+1)\mathrm{i}^m B_m Q_{mn} \mathrm{j}_n(\beta r) \frac{\mathrm{d}}{\mathrm{d}\theta} \mathrm{P}_n(\cos\theta), \quad (10)$$

The specific formula for Q_{mn} can be found in the appendix.

According to (4) - (6) and (9) - (10), the total velocity potential outside the sphere is obtained as

$$\begin{aligned}\phi = {} & A\sum_{n=0}^{\infty}(2n+1)\mathrm{i}^n \mathrm{j}_n(\alpha r)\mathrm{P}_n(\cos\theta) \\ & + AR_{\mathrm{s}}\sum_{n=0}^{\infty}\exp(\mathrm{i}2\alpha d)(-1)^n(2n+1)\mathrm{i}^n \mathrm{j}_n(\alpha r)\mathrm{P}_n(\cos\theta) \\ & + \sum_{n=0}^{\infty} A_n(2n+1)\mathrm{i}^n \mathrm{h}_n^{(1)}(\alpha r)\mathrm{P}_n(\cos\theta) \\ & + R_{\mathrm{s}}\sum_{n=0}^{\infty}\sum_{m=0}^{\infty}(-1)^m(2m+1)\mathrm{i}^m A_m Q_{mn} \mathrm{j}_n(\alpha r)\mathrm{P}_n(\cos\theta),\end{aligned} \quad (11)$$

$$\begin{aligned}\psi = {} & \sum_{n=0}^{\infty} B_n(2n+1)\mathrm{i}^n \mathrm{h}_n^{(1)}(\beta r)\frac{\mathrm{d}}{\mathrm{d}\theta}\mathrm{P}_n(\cos\theta) \\ & + R_{\mathrm{s}}\sum_{n=0}^{\infty}\sum_{m=0}^{\infty}(-1)^m(2m+1)\mathrm{i}^m B_m Q_{mn} \mathrm{j}_n(\beta r)\frac{\mathrm{d}}{\mathrm{d}\theta}\mathrm{P}_n(\cos\theta).\end{aligned} \quad (12)$$

For ease of calculation, introduce the definition:

$$a_n = A + AR_{\mathrm{s}}\exp(\mathrm{i}2\alpha d)(-1)^n + \frac{R_{\mathrm{s}}}{(2n+1)\mathrm{i}^n}\sum_{m=0}^{\infty}(-1)^m(2m+1)\mathrm{i}^m A_m Q_{mn}, \quad (13)$$

$$b_n = \frac{R_{\mathrm{s}}}{(2n+1)\mathrm{i}^n}\sum_{m=0}^{\infty}(-1)^m(2m+1)\mathrm{i}^m B_m Q_{mn}. \quad (14)$$

Substituting (13) and (14) into (11) and (12), the total velocity potential is obtained as

$$\phi = \sum_{n=0}^{\infty} a_n(2n+1)\mathrm{i}^n \mathrm{j}_n(\alpha r)\mathrm{P}_n(\cos\theta) + \sum_{n=0}^{\infty} A_n(2n+1)\mathrm{i}^n \mathrm{h}_n^{(1)}(\alpha r)\mathrm{P}_n(\cos\theta), \quad (15)$$

$$\psi = \sum_{n=0}^{\infty} b_n(2n+1)\mathrm{i}^n \mathrm{j}_n(\beta r)\frac{\mathrm{d}}{\mathrm{d}\theta}\mathrm{P}_n(\cos\theta) + \sum_{n=0}^{\infty} B_n(2n+1)\mathrm{i}^n \mathrm{h}_n^{(1)}(\beta r)\frac{\mathrm{d}}{\mathrm{d}\theta}\mathrm{P}_n(\cos\theta). \quad (16)$$

2.2 Scattering coefficients

The scattering coefficients A_n and B_n are determined by the boundary conditions on the surface of the spherical particle. In practical applications, such as ultrasonic drug delivery, many drug particles are liquid and elastic materials. Therefore, spherical particles of liquid and elastic materials are analyzed in this paper.

For a liquid spherical particle, the internal transmitted wave is only longitudinal wave. In the spherical coordinate system (r,θ,φ) the transmitted longitudinal wave is expressed as

$$\bar{\phi}=\sum_{n=0}^{\infty}C_n(2n+1)\mathrm{i}^n \mathrm{j}_n(k_\mathrm{L}r)\mathrm{P}_n(\cos\theta)\mathrm{e}^{-\mathrm{i}\omega t}. \tag{17}$$

At the interface between viscous fluid and liquid sphere $r=R$ the boundary conditions are satisfied:

$$\begin{aligned} v_r\,|_{r=R} &= \bar{v}_r\,|_{r=R}, \\ \sigma_{rr}\,|_{r=R} &= \bar{p}\,|_{r=R}, \\ \sigma_{r\theta}\,|_{r=R} &= 0, \end{aligned} \tag{18}$$

In which, $\bar{p}=\mathrm{i}\omega\rho_0\bar{\phi}$, v_r and $\bar{v}_r$ are the corresponding velocity components, σ_{rr}, $\bar{\sigma}_{rr}$, $\sigma_{r\theta}$, $\bar{\sigma}_{r\theta}$ are the corresponding stress tensor components, and the specific expressions are

$$\begin{aligned} v_r &= \frac{\partial\phi}{\partial r}+\frac{1}{r\sin\theta}\left[\frac{\partial(\psi\sin\theta)}{\partial\theta}\right], \\ \bar{v}_r &= \frac{\partial\bar{\phi}}{\partial r}+\frac{1}{r\sin\theta}\left[\frac{\partial(\bar{\psi}\sin\theta)}{\partial\theta}\right], \end{aligned} \tag{19}$$

$$\begin{aligned} \sigma_{rr} &= -p_1+2\mu'\frac{\partial v_r}{\partial r}+\lambda'\left(\frac{\partial v_r}{\partial r}+\frac{1}{r}\frac{\partial v_\theta}{\partial\theta}+\frac{2v_r}{r}+\frac{v_\theta\cot\theta}{r}\right), \\ \sigma_{r\theta} &= \frac{\mu'}{r}\left(r\frac{\partial v_\theta}{\partial r}-v_\theta+\frac{\partial v_r}{\partial\theta}\right), \end{aligned} \tag{20}$$

$$p_1=\rho_0\left(\frac{\lambda'+2\mu'}{\rho_0}\Delta-\frac{\partial}{\partial t}\right)\phi+\frac{\rho_0}{2c_0^2}\left(\frac{\partial\phi}{\partial t}\right)^2-\frac{1}{2}\rho_0(\nabla\phi)^2-\frac{\lambda'+2\mu'}{c_0^2}\frac{\partial\phi}{\partial t}\Delta\phi. \tag{21}$$

Considering the free sphere, $\partial\phi/\partial t$ in (21) should be performed in the fixed coordinate system in which the velocity potential is determined. That is

$$\frac{\partial\phi}{\partial t}=\frac{\mathrm{d}\phi}{\mathrm{d}t}-\boldsymbol{u}\cdot\nabla\phi, \tag{22}$$

where $\boldsymbol{u}$ is calculated by $m\dot{\boldsymbol{u}}=\iint_{S_0}\boldsymbol{\sigma}\mathrm{d}\boldsymbol{S}$, the stress tensor $\boldsymbol{\sigma}=\left(-p_1+\lambda'\nabla\cdot\boldsymbol{v}\right)\boldsymbol{E}+2\mu'\boldsymbol{e}$, $\boldsymbol{E}$ is the unit vector, the deformation tensor $\boldsymbol{e}=\left[\left(\nabla\boldsymbol{v}\right)+\left(\nabla\boldsymbol{v}\right)^\mathrm{T}\right]/2$, $m=4\pi R^3\rho_\mathrm{s}/3$ is the mass of the spherical particle, ρ_s is the particle density, $\boldsymbol{v}=\nabla\phi+\nabla\times\psi$ is the fluid velocity. Note that, when calculating the velocity of the sphere, it is only necessary to retain the first-order term by substituting (22) into (21) [23].

Incorporating (15)- (17) and (19)- (22) into (18), the scattering coefficient equations of a free liquid sphere near an impedance boundary in a viscous fluid are obtained:

$$[X]_{(3N)\times(3N)}\{I\}_{(3N)}=\{Y\}_{(3N)}, \tag{23}$$

$$\{I\}=\{A_0,\ A_1,\ \cdots,\ A_n;\ B_0,\ B_1,\ \cdots,\ B_n;\ \overline{A_0},\overline{A_1},\ \cdots,\ \overline{A_n}\}^{\mathrm{T}}, \tag{24}$$

The concrete expressions of the system of equations are

$$\begin{aligned}&\left\{\left[(2\mu'+\lambda')\frac{n(n-1)-\alpha^2R^2}{\alpha^2R^2}+\lambda'\frac{2n+1}{R^2}+\mathrm{i}\omega\rho_0\right]\mathrm{h}_n^{(1)}(\alpha R)+\frac{4\mu'\alpha}{R}\mathrm{h}_{n+1}^{(1)}(\alpha R)\right\}A_n\\&+\left\{\left[(2\mu'+\lambda')\frac{n(n-1)-\alpha^2R^2}{\alpha^2R^2}+\lambda'\frac{2n+1}{R^2}+\mathrm{i}\omega\rho_0\right]\mathrm{j}_n(\alpha R)+\frac{4\mu'\alpha}{R}\mathrm{j}_{n+1}(\alpha R)\right\}a_n\\&+\left[\frac{2(n+1)\lambda'+2(n-1)\mu'}{R^2}\mathrm{h}_n^{(1)}(\beta R)-(\mu'+\lambda')\frac{2\beta}{R}\mathrm{h}_{n+1}^{(1)}(\beta R)\right]\cdot n(n+1)B_n\\&+\left[\frac{2(n+1)\lambda'+2(n-1)\mu'}{R^2}\mathrm{j}_n(\beta R)-(\mu'+\lambda')\frac{2\beta}{R}\mathrm{j}_{n+1}(\beta R)\right]\cdot n(n+1)b_n-\mathrm{i}\omega\rho_s\mathrm{j}_n(k_LR)\overline{A_n}=0,\end{aligned}$$

$$\begin{aligned}&\frac{2\mu'}{\lambda'}\left[\frac{n-1}{R}\mathrm{h}_n^{(1)}(\alpha R)-\alpha\mathrm{h}_{n+1}^{(1)}(\alpha R)\right]A_n+\frac{2\mu'}{\lambda'}\left[\frac{n-1}{R}\mathrm{j}_n(\alpha R)-\alpha\mathrm{j}_{n+1}(\alpha R)\right]a_n\\&+\left\{\left[\frac{2(1-n)}{R}+\beta^2R\right]\mathrm{h}_n^{(1)}(\beta R)-2\beta\mathrm{h}_{n+1}^{(1)}(\beta R)\right\}B_n+\left\{\left[\frac{2(1-n)}{R}+\beta^2R\right]\mathrm{j}_n(\beta R)-2\beta\mathrm{j}_{n+1}(\beta R)\right\}b_n=0.\end{aligned}$$

For an elastic sphere, the sound wave is scattered by the sphere and refracted into transmitted longitudinal wave and transmitted transverse wave in the ball. The velocity potentials in the elastic sphere can be expressed in coordinate system $(r,\ \theta,\ \varphi)$ as

$$\overline{\phi}=\sum_{n=0}^{\infty}\overline{A_n}(2n+1)\mathrm{i}^n\mathrm{j}_n(k_Lr)\mathrm{P}_n(\cos\theta)\mathrm{e}^{-\mathrm{i}\omega t}, \tag{25}$$

$$\overline{\psi}=\sum_{n=0}^{\infty}\overline{B_n}(2n+1)\mathrm{i}^n\mathrm{j}_n(k_tr)\frac{\mathrm{d}}{\mathrm{d}\theta}\mathrm{P}_n(\cos\theta)\mathrm{e}^{-\mathrm{i}\omega t}, \tag{26}$$

where $k_L=\omega/c_L$ and $k_t=\omega/c_t$ are the wave numbers of transmitted longitudinal and transverse waves in the sphere respectively. $c_L=\sqrt{(\lambda+2\mu)/\rho_s}$ and $c_t=\sqrt{\mu/\rho_s}$ are the transmitted compressional and shear wave velocities. λ and μ are the Lamé constant, ρ_{s} is the density of the elastic sphere.

In the viscous fluid, the boundary conditions are applied at the surface of the sphere $(r = R)$

$$\begin{aligned} v_r |_{r=R} &= \overline{v_r} |_{r=R}, \\ v_\theta |_{r=R} &= \overline{v_\theta} |_{r=R}, \\ \sigma_{rr} |_{r=R} &= \overline{\sigma_{rr}} |_{r=R}, \\ \sigma_{r\theta} |_{r=R} &= \overline{\sigma_{r\theta}} |_{r=R}, \end{aligned} \tag{27}$$

where v_r, $\overline{v_r}$, σ_{rr}, $\sigma_{r\theta}$ are shown in (19) and (20). The specific expressions of v_θ, $\overline{v_\theta}$, $\overline{\sigma_{rr}}, \overline{\sigma_{r\theta}}$ are

$$\begin{aligned} v_\theta &= \frac{1}{r}\frac{\partial \phi}{\partial \theta} - \frac{1}{r}\frac{\partial (r\psi)}{\partial r}, \\ \overline{v_\theta} &= \frac{1}{r}\frac{\partial \overline{\phi}}{\partial \theta} - \frac{1}{r}\frac{\partial (r\overline{\psi})}{\partial r}, \end{aligned} \tag{28}$$

$$\begin{aligned} \overline{\sigma_{rr}} &= -\lambda k_{\mathrm{L}}^2 \overline{\phi} + 2\mu \left\{ \frac{\partial^2}{\partial r^2}\left[\overline{\phi} + \frac{\partial}{\partial r}(r\overline{\psi}) \right] + k_{\mathrm{t}}^2 (r\overline{\psi}) \right\}, \\ \overline{\sigma_{r\theta}} &= \mu \left\{ 2\frac{\partial}{\partial r}\left\{ \frac{1}{r}\frac{\partial}{\partial \theta}\left[\overline{\phi} + \frac{\partial}{\partial r}(r\overline{\psi}) \right] \right\} + k_{\mathrm{t}}^2 \frac{\partial \overline{\psi}}{\partial \theta} \right\}. \end{aligned} \tag{29}$$

Incorporating (15) - (16), (25) - (26), (19) - (20), and (28) - (29) into the boundary conditions (27), the scattering coefficient equations of a free elastic sphere near an impedance boundary in a viscous fluid can be obtained by calculation:

$$[X]_{(4N)\times(4N)} \{I\}_{4N} = \{Y\}_{4N}, \tag{30}$$

$$\{I\} = \{A_0,\ A_1,\ \cdots,\ A_n;\ B_0,\ B_1,\ \cdots,\ B_n;\ \overline{A_0}, \overline{A_1},\ \cdots,\ \overline{A_n};\ \overline{B_0}, \overline{B_1},\ \cdots,\ \overline{B_n}\}^{\mathrm{T}}. \tag{31}$$

The specific formula of this set of equations is

$$\left[n\mathrm{h}_n^{(1)}(\alpha R) - \alpha R \mathrm{h}_{n+1}^{(1)}(\alpha R) \right] A_n + \left[n\mathrm{j}_n(\alpha R) - \alpha R \mathrm{j}_{n+1}(\alpha R) \right] a_n - n(n+1)\mathrm{h}_n^{(1)}(\beta R) B_n - \mathrm{j}_n(\beta R) b_n$$
$$- \left[n\mathrm{j}_n(k_{\mathrm{L}} R) - k_{\mathrm{L}} R \mathrm{j}_{n+1}(k_{\mathrm{L}} R) \right] \overline{A_n} + n(n+1)\mathrm{j}_n(k_{\mathrm{t}} R) \overline{B_n} = 0,$$

$$\mathrm{h}_n^{(1)}(\alpha R) A_n + \mathrm{j}_n(\alpha R) a_n - \left[(n+1)\mathrm{h}_n^{(1)}(\beta R) + \beta R \mathrm{h}_{n+1}^{(1)}(\beta R) \right] B_n - \left[(n+1)\mathrm{j}_n(\beta R) + \beta R \mathrm{j}_{n+1}(\beta R) \right] b_n$$
$$- \mathrm{j}_n(k_{\mathrm{L}} R) \overline{A_n} + \left[(n+1)\mathrm{j}_n(k_{\mathrm{t}} R) + k_{\mathrm{t}} R \mathrm{j}_{n+1}(k_{\mathrm{t}} R) \right] \overline{B_n} = 0,$$

$$
\begin{aligned}
&2\mu'\left[(n-1)\mathrm{h}_n^{(1)}(\alpha R)-\alpha R\mathrm{h}_{n+1}^{(1)}(\alpha R)\right]A_n+2\mu'\left[(n-1)\mathrm{j}_n(\alpha R)+\alpha R\mathrm{j}_{n+1}(\alpha R)\right]a_n+\mu'\left[(2-2n^2-\beta^2R^2)\mathrm{h}_n^{(1)}(\beta R)-2\beta R\mathrm{h}_{n+1}^{(1)}(\beta R)\right]B_n\\
&+\mu'\left[(2-2n^2-\beta^2R^2)\mathrm{j}_n(\beta R)-2\beta R\mathrm{j}_{n+1}(\beta R)\right]b_n-2\mu\left[(n-1)\mathrm{j}_n(k_\mathrm{L}R)-k_\mathrm{L}R\mathrm{j}_{n+1}(k_\mathrm{L}R)\right]\overline{A_n}\\
&-\mu\left[(2-2n^2-k_\mathrm{t}^2R^2)\mathrm{j}_n(k_\mathrm{t}R)-2k_\mathrm{t}R\mathrm{j}_{n+1}(k_\mathrm{t}R)\right]\overline{B_n}=0,
\end{aligned}
$$

$$
\begin{aligned}
&\mu'\left\{\left[n(n-1)-\frac{1}{2}\alpha^2R^2\right]\mathrm{h}_n^{(1)}(\alpha R)+2\alpha R\mathrm{h}_{n+1}^{(1)}(\alpha R)\right\}A_n+\mu'\left\{\left[n(n-1)-\frac{1}{2}\alpha^2R^2\right]\mathrm{j}_n(\alpha R)+2\alpha R\mathrm{j}_{n+1}(\alpha R)\right\}a_n\\
&-\mu'\left[n(n+1)(n-1)\mathrm{h}_n^{(1)}(\beta R)-n(n+1)(\beta R)\mathrm{h}_{n+1}^{(1)}(\beta R)\right]B_n-\mu'\left[n(n+1)(n-1)\mathrm{j}_n(\beta R)-n(n+1)(\beta R)\mathrm{j}_{n+1}(\beta R)\right]b_n\\
&-\mu\left\{\left[n(n-1)-k_\mathrm{L}^2R^2-\frac{\lambda}{2\mu}k_\mathrm{L}^2R^2\right]\mathrm{j}_n(k_\mathrm{L}R)+k_\mathrm{L}R\mathrm{j}_{n+1}(k_\mathrm{L}R)\right\}\overline{A_n}+\mu\left[n(n+1)(n-1)\mathrm{j}_n(k_\mathrm{t}R)-n(n+1)(k_\mathrm{t}R)\mathrm{j}_{n+1}(k_\mathrm{t}R)\right]\overline{B_n}=0.
\end{aligned}
$$

2.3 Acoustic radiation force

The acoustic radiation force on a particle in an acoustic field can be expressed as。

$$
\boldsymbol{F}=\left\langle\iint_{S(t)}\boldsymbol{\sigma}\mathrm{d}\boldsymbol{S}\right\rangle, \tag{32}
$$

where $\boldsymbol{\sigma}=\left(-p_1+\lambda'\nabla\cdot\boldsymbol{v}\right)\boldsymbol{E}+2\mu'\boldsymbol{e}$. Combine (21), (32) is written as。

$$
\boldsymbol{F}=\left\langle\iint_{S(t)}\left\{\left[-\left(\rho_0(\frac{\lambda'+2\mu'}{\rho_0}\Delta-\frac{\partial}{\partial t})\phi+\frac{\rho_0}{2c_0^2}(\frac{\partial\phi}{\partial t})^2-\frac{1}{2}\rho_0(\nabla\phi)^2-\frac{\lambda'+2\mu'}{c_0^2}\frac{\partial\phi}{\partial t}\Delta\phi\right)+\lambda'\nabla\cdot\boldsymbol{v}\right]\boldsymbol{E}+2\mu'\boldsymbol{e}\right\}\mathrm{d}\boldsymbol{S}\right\rangle, \tag{33}
$$

where $\langle\cdot\rangle$ denoting the time average, $\mathbf{E}$ is a unit vector, $\mathbf{e}$ is the deformation tensor, $\mathrm{d}\mathbf{S}$ is a bin, $S(t)$ is the surface of the spherical particle, which is a function of time. A sound wave propagates in a viscous fluid, acts on a particle, and produces momentum transfer between the particles. According to the Leibniz-Reynolds transmission theorem [20], the rate of change of momentum within the volume $V(t)$ defined by surface $S(t)$ is equal to the rate of change of momentum in the volume under the action of the sound field plus the net transport of momentum through the particle surface. Therefore, in order to solve the problem that the integral surface is a function of time, Yosioka et al. [24] transformed the integral surface $S(t)$ into the initial surface area of the particle S_0, and corrected the ARF by adding a momentum flux term $\rho_0\boldsymbol{u}\cdot\nabla\phi$. Let $\partial\phi/\partial t=\mathrm{d}\phi/\mathrm{d}t-\boldsymbol{u}\cdot\nabla\phi$, (33) can be rewritten as

$$
\begin{aligned}
\boldsymbol{F}=&\left\langle\iint_{S_0}\left\{\left[-\left(\rho_0\left(\frac{\lambda'+2\mu'}{\rho_0}\Delta\right)\phi+\frac{\rho_0}{2c_0^2}\left(\frac{\partial\phi}{\partial t}\right)^2-\frac{1}{2}\rho_0(\nabla\phi)^2-\frac{\lambda'+2\mu'}{c_0^2}\frac{\partial\phi}{\partial t}\Delta\phi\right)+\lambda'\nabla\cdot\boldsymbol{v}\right]\boldsymbol{E}+2\mu'\boldsymbol{e}\right\}\mathrm{d}\boldsymbol{S}\right\rangle\\
&+\left\langle\iint_{V(t)}\rho_0\frac{\partial\phi}{\partial t}\boldsymbol{E}\mathrm{d}\boldsymbol{V}\right\rangle,
\end{aligned} \tag{34}
$$

In which, $V(t)$ is the volume defined by surface $S(t)$. Combined with the following formula [20]:

$$
\iint_{V(t)}\frac{\partial\phi}{\partial t}\mathrm{d}\boldsymbol{V}=\iint_{V(t)}\frac{\mathrm{d}\phi}{\mathrm{d}t}\mathrm{d}\boldsymbol{V}-\iint_{S_0}\boldsymbol{u}\cdot\nabla\phi\mathrm{d}\boldsymbol{S}, \tag{35}
$$

$$\left\langle \iint_{V(t)} \frac{\mathrm{d}\phi}{\mathrm{d}t} \mathrm{d}\boldsymbol{V} \right\rangle = 0, \tag{36}$$

One can obtain:

$$\begin{aligned}
\boldsymbol{F} &= \left\langle \iint_{S_0} \left\{ \left[-\left(\rho_0 \left(\frac{\lambda' + 2\mu'}{\rho_0} \Delta \right) \phi + \frac{\rho_0}{2c_0^2} \left(\frac{\partial \phi}{\partial t} \right)^2 - \frac{1}{2} \rho_0 (\nabla \phi)^2 - \frac{\lambda' + 2\mu'}{c_0^2} \frac{\partial \phi}{\partial t} \Delta \phi \right) + \lambda' \nabla \cdot \boldsymbol{v} \right] \boldsymbol{E} + 2\mu' \boldsymbol{e} \right\} \mathrm{d}\boldsymbol{S} \right\rangle \\
&\quad - \left\langle \iint_{S_0} \rho_0 \boldsymbol{u} \cdot \nabla \phi \boldsymbol{E} \mathrm{d}\boldsymbol{S} \right\rangle \\
&= \left\langle \iint_{S_0} \left\{ \left[-\left(\rho_0 \left(\frac{\lambda' + 2\mu'}{\rho_0} \Delta + \boldsymbol{u} \cdot \nabla \right) \phi + \frac{\rho_0}{2c_0^2} \left(\frac{\partial \phi}{\partial t} \right)^2 - \frac{1}{2} \rho_0 (\nabla \phi)^2 - \frac{\lambda' + 2\mu'}{c_0^2} \frac{\partial \phi}{\partial t} \Delta \phi \right) + \lambda' \nabla \cdot \boldsymbol{v} \right] \boldsymbol{E} + 2\mu' \boldsymbol{e} \right\} \mathrm{d}\boldsymbol{S} \right\rangle \\
&= \left\langle \iint_{S_0} \left[(-p_1 + \lambda' \nabla \cdot \boldsymbol{v}) \boldsymbol{E} + 2\mu' \boldsymbol{e} \right] \mathrm{d}\boldsymbol{S} \right\rangle \\
&= \left\langle \iint_{S_0} \boldsymbol{\sigma} \mathrm{d}\boldsymbol{S} \right\rangle,
\end{aligned} \tag{37}$$

At this point, the expression for p_1 has been combined with $\partial\phi/\partial t = \mathrm{d}\phi/\mathrm{d}t - \boldsymbol{u} \cdot \nabla\phi$ and transformed into:

$$p_1 = \rho_0 \left(\frac{\lambda' + 2\mu'}{\rho_0} \Delta + \boldsymbol{u} \cdot \nabla \right) \phi + \frac{\rho_0}{2c_0^2} \left(\frac{\partial \phi}{\partial t} \right)^2 - \frac{1}{2} \rho_0 (\nabla \phi)^2 - \frac{\lambda' + 2\mu'}{c_0^2} \frac{\partial \phi}{\partial t} \Delta \phi \cdot$$

The second order term in the p_1 should be taken into account in the calculation of the ARF.

The (37) can be written in component form as

$$F_i = \left\langle \iint_{S_0} \sigma_{ik} n_k \mathrm{d}S \right\rangle, \tag{38}$$

Where n_k is the component of the unit vector in the outward direction of the spherical particle bin $\mathrm{d}S$ in the direction of k, and σ_{ik} is the stress tensor.

In a bounded viscous fluid, when a plane wave is incident along the direction perpendicular to the boundary, the only ARF acting on a free spherical particle in the fluid is along the Ox axis, and the projection of (38) in the direction of the x axis is

$$\begin{aligned}
F_x &= \left\langle \iint_{S_0} (\sigma_{rr} \cos\theta - \sigma_{r\theta} \sin\theta) \mathrm{d}S \right\rangle \\
&= \left\langle \int_0^{\pi} \int_0^{2\pi} (\sigma_{rr} \cos\theta - \sigma_{r\theta} \sin\theta) R^2 \sin\theta \mathrm{d}\theta \mathrm{d}\varphi \right\rangle \\
&= \left\langle 2\pi R^2 \int_0^{\pi} (\sigma_{rr} \cos\theta - \sigma_{r\theta} \sin\theta) \sin\theta \mathrm{d}\theta \right\rangle.
\end{aligned} \tag{39}$$

For the convenience of calculation, the total velocity potential (15) and (16) outside the spherical particle are rewritten as

$$\begin{aligned}\phi &= \sum_{n=0}^{\infty}(G_n + \mathrm{i}L_n)\mathrm{P}_n(\cos\theta)\mathrm{e}^{-\mathrm{i}\omega t},\\ \psi &= \sum_{n=0}^{\infty}(M_n + \mathrm{i}N_n)\frac{\mathrm{d}}{\mathrm{d}\theta}\mathrm{P}_n(\cos\theta)\mathrm{e}^{-\mathrm{i}\omega t},\end{aligned} \tag{40}$$

In which,

$$\begin{aligned}G_n &= \mathrm{Re}\{[a_n \mathrm{j}_n(\alpha r) + A_n \mathrm{h}_n^{(1)}(\alpha r)](2n+1)\},\\ L_n &= \mathrm{Im}\{[a_n \mathrm{j}_n(\alpha r) + A_n \mathrm{h}_n^{(1)}(\alpha r)](2n+1)\},\\ M_n &= \mathrm{Re}\{[b_n \mathrm{j}_n(\beta r) + B_n \mathrm{h}_n^{(1)}(\beta r)](2n+1)\},\\ N_n &= \mathrm{Im}\{[b_n \mathrm{j}_n(\beta r) + B_n \mathrm{h}_n^{(1)}(\beta r)](2n+1)\}.\end{aligned}$$

Substituting (40) into (39), combined with the recursion formula of spherical Bessel functions and the properties of Legendre functions, the axial ARF of a free spherical particle in a bounded viscous fluid is derived as

$$\begin{aligned}\langle F_x \rangle &= -6\frac{\rho_0^2}{\rho_1}\pi\left\{\frac{1}{3}\left[(2N_1 - L_1)G_0 + (G_1 - 2M_1)L_0\right] + \frac{2}{5}\left[(2N_1 - L_1)G_2 + (G_1 - 2M_1)L_2\right]\right\}\\ &-\rho_0\pi\left(\frac{\omega R}{c_0}\right)^2 \sum_{n=0}^{\infty}\frac{n+1}{(2n+1)(2n+3)}(G_n G_{n+1} + L_n L_{n+1}) + \rho_0\pi\sum_{n=0}^{\infty}\frac{n(n+2)(n+1)}{(2n+1)(2n+3)}\left[(n+1)^2(M_n M_{n+1} + N_n N_{n+1}) + (G_n G_{n+1} + L_n L_{n+1})\right]\\ &+\frac{2\pi R^2(\lambda' + 2\mu')\rho_0\omega^3}{\rho_0{}^2 c_0^2 + \omega^2(\lambda' + 2\mu')^2}\sum_{n=0}^{\infty}\frac{n+1}{(2n+1)(2n+3)}\left[\rho_0(G_n L_{n+1} - L_n G_{n+1}) + (\lambda' + 2\mu')\omega(G_n G_{n+1} + L_n L_{n+1})\right].\end{aligned} \tag{41}$$

Depending on the fluid viscosity, particle material, particle position, boundary reflection coefficient, etc., the scattering coefficient A_n and B_n change, and the ARF varies.

3. Numerical simulation

In order to expand the basic theory of acoustic manipulation of a free spherical particle in a bounded viscous fluid, and analyze the effects of fluid viscosity, particle material, particle position, and the boundary on the ARF acting on a free spherical particle in a plane wave acoustic field, polyethylene (PE), a common biomaterial for drug carrier, is selected to carry out numerical analysis. To analyze the influence of particle material on the ARF, the ARFS of an oleic acid and a polymethyl methacrylate (PMMA) particle are numerically calculated. The volume expansion of the fluid is not considered in the numerical simulation, and the second viscosity coefficient $\eta' = 0$ is taken. The acoustic parameters of the particle material and the fluid are given by Tab. 1 and Tab. 2.

Table 1. Physical parameters of free spherical particles [25,26].

Material	Density /(kg m^{-3})	longitudinal wave velocity /(m s^{-1})	Transverse wave velocity /(m s^{-1})
Oleic acid	938	1450	—
Polyethylene (PE)	957	2430	950
Polymethyl methacrylate (PMMA)	1190	2690	1340

Table 2. Acoustic parameters of fluids [18].

Fluid	Density /(kg m^{-3})	Sound velocity /(m s^{-1})	Dynamic viscosity μ'/(Pa·s)
Water	1000	1500	0.001
Glycerin	1260	1900	1.48

3.1 Effect of fluid viscosity on ARF

In order to study the effect of fluid viscosity on the ARF, a PE sphere with radius R=0.5mm is considered, which is freely placed in the fluid at a distance d=4R from the rigid boundary (R_s=1). The ARFs under different δ/R (boundary layer thickness-particle radius ratio) and ideal fluid conditions are shown in Fig. 2.

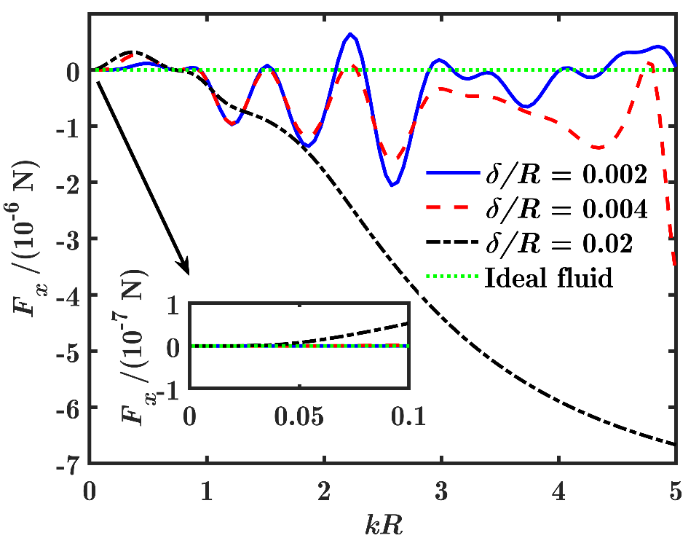

Figure 2. ARFs for a free PE sphere versus *kR* at different δ/R.

It can be seen from the Fig. 2 that with the increase of the δ/R, the ARF first increases and then decreases, and when the δ/R is small, there are more peaks and troughs in the ARF curve. Because, as the δ/R increases, the boundary layer becomes thicker and thicker, the dissipation and attenuation of the sound wave become greater, and the corresponding resonance peak is broadened. At the same time, comparing the two cases of viscous fluid and ideal fluid, it can be found that when $kR \ll 1$, the influence of fluid viscosity is small, and the viscous effect is almost negligible; However, when the kR is large, the amplitude of the ARF on the particle in the viscous fluid is much larger than that in the ideal fluid, and the influence of the fluid viscosity on the ARF is great and cannot be ignored. In order to show the comparison results of the two cases more simply, the values of the ARFs are given in Tab. 3 when the kR is 1.0×10^{-4}, 1.0×10^{-2}, 1.0×10^{-1}, 1.0, 5.0. From Tab. 3, it can be found that when $kR = 1.0 \times 10^{-4}$, 1.0×10^{-2}, the effect of fluid viscosity on ARF can be ignored; However, for $kR = 1.0 \times 10^{-1}$, 1.0, 5.0, the effect of fluid viscosity increases the ARF by several orders of magnitude.

Table 3. Comparisons of the ARFs on a free PE sphere in a viscous and an ideal fluid.

Fluid		kR				
		1.0×10^{-4}	1.0×10^{-2}	1.0×10^{-1}	1.0	5.0
Viscous fluid	δ/R=0.002	4.8×10^{-12} N	5.2×10^{-12} N	1.1×10^{-10} N	-2.1×10^{-7} N	5.6×10^{-8} N
	δ/R=0.004	4.8×10^{-12} N	5.2×10^{-12} N	1.4×10^{-9} N	-2.2×10^{-7} N	-3.7×10^{-6} N
	δ/R=0.02	4.8×10^{-12} N	5.2×10^{-12} N	5.3×10^{-8} N	-2.7×10^{-7} N	-6.7×10^{-6} N
ideal fluid	$\lambda'=\mu'=0$	4.8×10^{-12} N	5.2×10^{-12} N	1.2×10^{-11} N	1.7×10^{-13} N	6.2×10^{-14} N

3.2 ARFs of particles of different materials

The material of the particle is also an important factor affecting the ARF. In order to analyze the influence of particle material, the elastic material polymethylmethacrylate (PMMA) and the liquid material oleic acid are also selected in this numerical simulation. The parameters d=4R and R_s=1 are selected. The ARFs of a free spherical particle with radius R=0.5mm in a low viscosity fluid (water) are given in Fig. 3. Fig. 3 shows that the ARF is significantly affected by the material of the sphere. The ARFs of the elastic materials PE and PMMA are generally larger than that of the liquid material oleic acid sphere, and the oscillation phenomenon of ARF are more obvious, with more peaks and troughs; The amplitude of ARF of PMMA is slightly larger than that of PE. This is because the momentum transfer of sound waves between elastic materials is greater than that between sound waves and liquids.

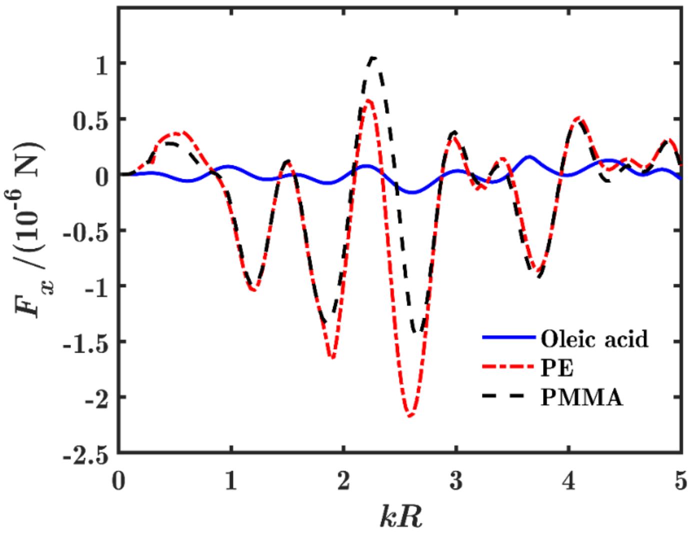

Figure 3. ARFs for a free sphere with different materials versus *kR* in the low viscosity liquid (water).

3.3 Effect of impedance boundary on ARF

The effect of impedance boundary on the ARF of PE sphere is shown in the Fig. 4. In the numerical simulation, the parameters d=4R and R=0.5 mm are selected, and the particle is considered to be freely placed in a low viscosity fluid (water).

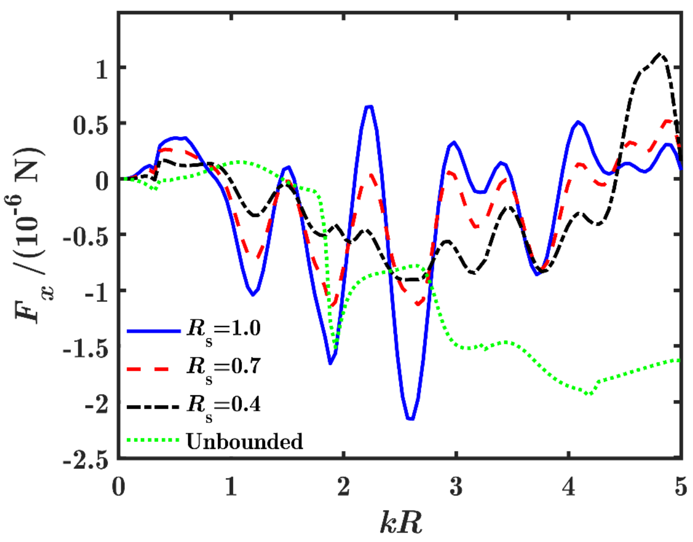

Figure 4. ARFs for a free PE sphere versus *kR* in the low viscosity liquid (water) with different R_s.

It is worth noting that the addition of the impedance boundary makes the ARF curve change compared with the unbounded space. In addition to the change of the oscillation phenomenon of the ARF, the amplitude increases with the increase of the boundary reflection coefficient in the case of boundary. More oscillations occur because of the interaction of the sphere with the waves reflected from the boundary. In addition, the resonance frequency of the ARF function curve does not change with the change of the reflection coefficient.

3.4 Effect of particle position on ARF

The position of the sphere near the boundary is also a factor that cannot be ignored, and the ARFs on the PE sphere placed at different positions are presented in the Fig. 5. The Fig. 5 represents the ARF at three different positions: small (d=R), medium (d=2R) and large (d=4R), and the particle radius is R=0.5 mm and R_s=1.

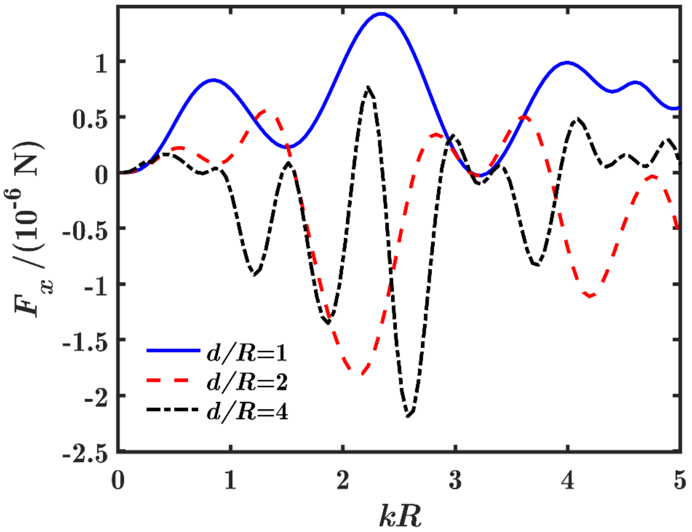

Figure 5. ARFs for a free PE sphere in the low viscosity liquid (water) versus *kR* at different *d*.

It can be seen that the oscillation of the ARF is mainly affected by the different positions of the sphere. With the increase of the position d/R, the peak value of the ARF changes more dramatically, and there are more peaks and troughs. The main reason is that the interaction between the scattered wave of the particle and the reflected wave from the boundary leads to the oscillation. It is worth mentioning that this is different from the effect of the reflection coefficient, which mainly affects the amplitude of the ARF, while the change of the sphere position mainly affects the period of the ARF.

4. Conclusion

In this paper, a general formula for the ARF of a free spherical particle in a viscous fluid near the boundary is given when a plane wave is incident normally. In the calculation, the dynamic equation of the particle is used as the correction term of the ARF. The effects of fluid viscosity, particle material, particle position and boundary on the ARF are considered, and the variation of the ARF under different conditions is intuitively displayed by numerical simulation. The results show that with the increase of fluid viscosity, the peaks and troughs of the ARF curve decrease, and the resonance peaks are broadened; The ARF is significantly affected by the spherical material, and the oscillation of the ARF of the elastic material is more obvious than that of the spherical particle of the liquid material; With the increase of the reflection coefficient of the impedance boundary, the amplitude of the ARF increases, but the resonance frequency of the ARF function curve is not affected; The oscillation period of the ARF is mainly affected by the different positions of the sphere. With the increase of the distance from the boundary, there are more peaks and troughs in the ARF curve. The method in this paper can also be extended to ellipsoidal and other shaped particles or the existence of multiple target particles, so as to facilitate more accurate targeted manipulation of cells, bacteria, drugs, etc. in the future.

Appendix

The concrete expression of Q_{mn} is

$$Q_{mn} = \sqrt{(2n+1)(2m+1)}\mathrm{i}^{m-n} \sum_{\sigma=|m-n|}^{m+n} (-1)^{\sigma} \mathrm{i}^{\sigma} b_{\sigma}^{mn} \mathrm{h}_{\sigma}^{(1)}(\alpha d),$$

In which,

$$b_{\sigma}^{mn} = (mn00|\sigma 0)^2,$$

$$(mn00|\sigma 0) = \frac{(-1)^{q+\sigma} q!}{(q-n)!(q-m)!(q-\sigma)!} \times \sqrt{\frac{2\sigma+1}{(2q+1)!}(2q-2n)!(2q-2m)!(2q-2\sigma)!}.$$

For even q, $(mn00|\sigma 0) = (\sigma + m + n)/2$; for odd q, then $(mn00|\sigma 0) = 0$.

References

[1] Ozcelik A, Rufo J, Guo F, Gu Y Y, Li P, Lata J, Huang T J 2018 *Nat. Methods* **15** 1021

[2] Meng L, Cai F Y, Li F, Zhou W, Niu L L, Zheng H R 2019 *J. Phys. D Appl. Phys.* **52** 273001

[3] King L V 1934 *Proc. R. Soc. London* **147** 861

[4] Hasegawa T, Yosioka K 1969 *J. Acoust. Soc. Am.* **46** 5

[5] Marston P L 2006 *J. Acoust. Soc. Am.* **120** 3518

[6] Gong Z X, Marston P L, Li W 2019 *Phys. Rev. E* **99** 063004

[7] Zang Y C, Su C, Wu P F, Lin W J 2022 *Acta Phys. Sin.* **71** 104302

[8] Li S Y, Shi J Y, Zhang X F, Zhang G B 2019 *J. Acoust. Soc. Am.* **145** 5

[9] Azarpeyvand M, Azarpeyvand M 2013 *J. Sound Vib.* **332** 9

[10] Zang Y C, Lin W 2019 *Results Phys.* **16** 102847

[11] Mitri F G 2009 *Ultrasonics* **49** 794

[12] Marston P L 2009 *J. Acoust. Soc. Am.* **125** 6

[13] Gong M Y, Shi M J, Li Y Y, Xu X, Fei Z H, Qiao Y P, Liu J H, He A J, Liu X Z 2023 *Phys. Fluids* **35** 057108

[14] Gong M Y, Xu X, Qiao Y P, Liu J H, He A J, Liu X Z 2024 *Chin. Phys. B* **33** 014302

[15] Gaunaurd G C, Huang H 1991 *J. Acoust. Soc. Am.* **96** 2526

[16] Miri A K, Mitri F G 2011 *Ultrasound Med. Biol.* **37** 2

[17] Westervelt P J 1951 *J. Acoust. Soc. Am.* **23** 3

[18] Doinikov A A 1994 *J. Fluid Mech.* **267** 1

[19] Qiao Y P, Gong M Y, Wang H B, Lan J, Liu T, Liu J H, Mao Y W, He A J, Liu X Z 2021 *Phys. Fluids* **33** 047107

[20] Kundu P K, Cohen I M 2002 *Fluid Mechanics* (San Diego: Academic Press) p78, p96

[21] Huang H, Gaunaurd G C 1997 *Int. J. Solids Struct.* **34** 591

[22] Hasheminejad S M 2001 *Acta Acust. United Ac.* **87** 4

[23] Embleton T F W 1954 *J. Acoust. Soc. Am.* **26** 1

[24] Yosioka K, Kawasima Y 1955 *Acta. Acust. United Ac.* **5** 3

[25] Wang H B, Gao S, Qiao Y P, Liu J H, Liu X Z 2019 *Phys. Fluids* **31** 047103

[26] Hartman B, Jarzynski J 1972 *J. Appl. Phys.* **43** 11